8th GRACM International Congress on Computational Mechanics
Volos, 12 July – 15 July 2015

VISCOELASTIC SIMULATIONS WITH INTEGRAL MODELS AT EXTREMELY HIGH SHEAR RATES

Evan Mitsoulis

School of Mining Engineering and Metallurgy
National Technical University of Athens
Zografou, GR-15780, Greece
e-mail: mitsouli@metal.ntua.gr ; web page: http://www.metal.ntua.gr/index.pl/mitsoulis

Keywords: Integral Models, Viscoelasticity, High Shear Rates, Convergence of the Simulations.

Abstract. *Viscoelasticity is important in many polymer processes, where the material is highly viscous and elastic, as measured in rheometrical experiments. A polypropylene nanocomposite is studied. This material has shown experimentally high viscoelasticity. To model this behavior, an integral viscoelastic model of the K-BKZ type with multiple relaxation times has been used. The model is used first to fit the rheological data and then to simulate flow through injection molding dies, where apparent shear rates reach 1,000,000 1/s. At such extremely high shear rates, it was impossible in the past to achieve convergence. In the present work, a careful continuation study has been done to increase slowly the flow rate (hence the apparent shear rate) and achieve convergence up to the limits of experiments. The results for the pressure drop in the system are consistent with the experimental findings.*

1 INTRODUCTION

Viscoelastic materials have properties combining viscous effects and elastic effects [1]. When they flow they show interesting phenomena not seeing with purely viscous fluids. These are called *viscoelastic phenomena* and they come under the scientific section of *non-Newtonian Fluid Mechanics*. The most important viscoelastic materials are polymer solutions and melts and rubber, because of the macromolecular structure in the chemistry of these materials [1].

Modeling of viscoelasticity is not easy because the constitutive equations that describe the behavior of the viscoelastic materials are complicated functions and functionals of the stress tensor. The science that deals with the development and solution of the constitutive equations is called *computational rheology* [2]. A plethora of constitutive equations exists that has developed models of differential and integral types. Among the most successful differential models are the Phan-Thien–Tanner (PTT) [2], Giesekus [3], and Pom-Pom models [4]. Among the most successful integral models are the K-BKZ models [5,6], and its variants the Wagner model [7] and the PSM model [8].

The solution of these models had been plagued early on (in the 1980's) by lack of convergence for relatively low elasticity levels [2]. These levels were determined by appropriate dimensionless numbers, such as the Deborah (*De*) and the Weissenberg (*Ws*) numbers. While these numbers go in real flow problems from 2 to 5, in the early simulations convergence was lost at values around 1. This was called the "High Weissenberg Value Problem" [9]. The solution to this problem came about in the late 1980's with the imposition in the numerical methods as solution variables the velocities, pressures, stresses and strain rates (DEVSS method), Streamline-Upwind Petrov-Galerkin (SUPG) techniques to deal with the convective nature of the viscoelastic flows [10], and streamline integration for integral models [11].

Since the 1990's many problems have been solved with the above mentioned constitutive equations, but a special mention has to be made to the integral constitutive equation of the K-BKZ type with the PSM damping function [8], which has been used by many researchers around the world for the solution of real problems for real polymeric fluids (solutions and melts) used in polymer processing [12]. Thus, it was possible in the 1990's to solve benchmark problems, such as flows through contractions and extrudate swell [13], for apparent shear rates U/R up to 10 s^{-1}, where U is the average velocity of the fluid and R is a characteristic length, usually the tube (die) radius. In the 2000's, the simulations went even higher and reached apparent shear rates of 1000 s^{-1} [14]. The reasons for this type of convergence at such high apparent shear rates were a careful continuation strategy of incrementing the shear rates slowly from very low values (1 s^{-1}) to higher ones as needed.

New experiments with rubber and polypropylene nanocomposites showed that it was possible in injection molding dies to reach apparent shear rates of 1,000,000 s^{-1}, with good results [15]. It was, therefore, a challenge

for the computational community to see whether it was possible to do such viscoelastic simulations and to try to reach these extremely high apparent shear rates, something that has never been done before. This is the subject matter of the present work.

2 RHEOLOGICAL CHARACTERIZATION

2.1 Material Used

The material used is a polypropylene nanocomposite. This material is first rheologically characterized in the molten state. First, an Anton Paar MCR-501 device was used in the parallel-plate geometry to determine its linear viscoelastic moduli over a wide range of temperatures from 200ºC to 230ºC [15].

2.2 Capillary Flow Testing

An Instron capillary rheometer (constant piston speed) was used to determine the entrance pressure (known also as the Bagley method) and the viscosity as a function of the wall shear stress, σ_w, and apparent shear rate, $\dot{\gamma}_A = 32Q/\pi D^3$, where Q is the volumetric flow rate and D is the capillary diameter. Two dies (an orifice die with D=0.1 cm and L/D=0.2 with a reservoir of D_{res}=1.2 cm, and a long die with L/D=20) were also used to determine directly the entrance pressure as a function of the apparent shear rate. The experiments were performed at various temperatures, from 200ºC to 230ºC for the polypropylene nanocomposite [15].

3 GOVERNING EQUATIONS AND RHEOLOGICAL MODELING

We consider the conservation equations of mass, momentum, and energy for incompressible fluids under non-isothermal, creeping, steady flow conditions. These are written as [1-3]:

$$\nabla \cdot \overline{u} = 0 \tag{1}$$

$$0 = -\nabla p + \nabla \cdot \overline{\overline{\tau}} \tag{2}$$

$$\rho C_p \overline{u} \cdot \nabla T = k\nabla^2 T + \overline{\overline{\tau}} : \nabla \overline{u} \tag{3}$$

where ρ is the density, $\overline{u}$ is the velocity vector, p is the pressure, $\overline{\overline{\tau}}$ is the extra stress tensor, T is the temperature, C_p is the heat capacity, and k is the thermal conductivity.

The viscous stresses are given for inelastic non-Newtonian fluids by the relation [1-3]:

$$\overline{\overline{\tau}} = \eta\left(|\dot{\gamma}|\right)\overline{\overline{\dot{\gamma}}} \tag{4}$$

where $\eta\left(|\dot{\gamma}|\right)$ is the apparent non-Newtonian viscosity, which is a function of the magnitude $|\dot{\gamma}|$ of the rate-of-strain tensor $\overline{\overline{\dot{\gamma}}} = \nabla\overline{u} + \nabla\overline{u}^T$, which is given by:

$$|\dot{\gamma}| = \sqrt{\frac{1}{2}II_{\dot{\gamma}}} = \left(\frac{1}{2}\left(\overline{\overline{\dot{\gamma}}} : \overline{\overline{\dot{\gamma}}}\right)\right)^{1/2} \tag{5}$$

where $II_{\dot{\gamma}}$ is the second invariant of $\overline{\overline{\dot{\gamma}}}$

$$II_{\dot{\gamma}} = \left(\overline{\overline{\dot{\gamma}}} : \overline{\overline{\dot{\gamma}}}\right) = \sum_i \sum_j \dot{\gamma}_{ij}\dot{\gamma}_{ij} \tag{6}$$

To evaluate the role of viscoelasticity in the prediction of entrance pressure, it is instructive to consider first purely viscous models in the simulations. Namely, the Cross model was used to fit the shear viscosity data of the polypropylene nanocomposite. The Cross model is written as [1-3]:

$$\eta = \frac{\eta_0}{1 + (\lambda\dot{\gamma})^{1-n}} \tag{7}$$

where η_0 is the zero-shear-rate viscosity, λ is a time constant, and n is the power-law index. The fitted viscosity of the polypropylene nanocomposite by eqn (7) is plotted in Figure 1, while the parameters of the model are listed in Table 1. We observe that the material is very shear-thinning for shear rates above 1 s^{-1} giving a low power-law index n=0.2. The Cross model fits the data well over the range of experimental results.

Parameter	Value at 200ºC	Value at 215ºC	Value at 230ºC
η_0	11525 Pa·s	7228.4 Pa·s	4720.6 Pa·s
λ	0.312 s	0.194 s	0.121 s
n	0.20	0.20	0.19

Table 1 : Parameters of the Cross model (eqn 7) fitting the viscosity data of polypropylene nanocomposite

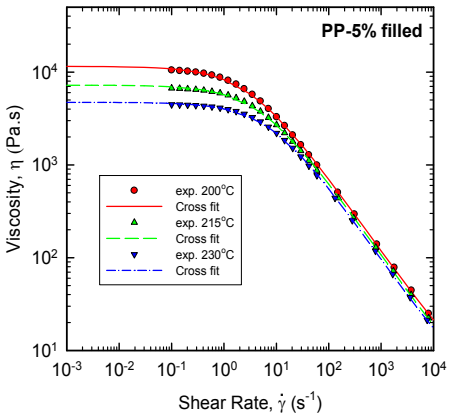

Figure 1. Shear viscosity data of the polypropylene nanocomposite and its best fit with the Cross model (eqn 7)

Viscoelasticity is included in the present work via an appropriate rheological model for the stresses. This is a K-BKZ equation proposed by Papanastasiou et al. [8] and modified by Luo and Tanner [16]. This is written as:

$$\boldsymbol{\tau} = \frac{1}{1-\theta}\int_{-\infty}^{t}\sum_{k=1}^{N}\frac{a_k}{\lambda_k}\exp\left(-\frac{t-t'}{\lambda_k}\right)\frac{\alpha}{(\alpha-3)+\beta I_{\boldsymbol{C}^{-1}}+(1-\beta)I_{\boldsymbol{C}}}\left[\boldsymbol{C}_t^{-1}(t')+\theta\boldsymbol{C}_t(t')\right]\mathrm{d}t' \qquad (8)$$

where t is the current time, λ_k and a_k are the relaxation times and relaxation modulus coefficients, N is the number of relaxation modes, α and β are material constants, and $I_{\boldsymbol{C}}$, $I_{\boldsymbol{C}^{-1}}$ are the first invariants of the Cauchy-Green tensor $\boldsymbol{C}_t$ and its inverse $\boldsymbol{C}_t^{-1}$, the Finger strain tensor. The material constant θ is given by

$$\frac{N_2}{N_1} = \frac{\theta}{1-\theta} \qquad (9)$$

where N_1 and N_2 are the first and second normal stress differences, respectively. It is noted that θ is not zero for polymer melts, which possess a non-zero second normal stress difference. Its usual range is between –0.1 and –0.2 in accordance with experimental findings [1,2,13].

As discussed above, experiments were performed in the parallel-plate and capillary rheometers for the polypropylene nanocomposite to rheologically characterize it. Figure 2a plots the dynamic moduli G' and G'' at the three temperatures of 200°C, 215°C, and 230°C. The model predictions obtained by fitting the experimental data to eqn (8) with a spectrum of relaxation times, λ_k, and coefficients, a_k, determined by a non-linear regression package [17], are also plotted. The parameters found from the fitting procedure are listed in Table 2. The relaxation spectrum is used to find the average relaxation time, $\bar{\lambda}$, and zero-shear-rate viscosity, η_0, according to the formulas:

$$\bar{\lambda} = \frac{\sum_{k=1}^{N} a_k \lambda_k^2}{\sum_{k=1}^{N} a_k \lambda_k} \qquad (10)$$

$$\eta_0 = \sum_{k=1}^{N} a_k \lambda_k \qquad (11)$$

Figure 2b plots a number of calculated and experimental material functions for the polypropylene nanocomposite at the three temperatures. Namely, data for the shear viscosity, η_S, the elongational viscosity, η_E, and the first normal stress difference, N_1, are plotted as functions of corresponding rates (shear or extensional). The parameter β that controls the calculated elongational viscosity was fitted by using the extensional behaviour of the melt, which is essentially equal to $3\eta^+$. It can be seen that the overall rheological representation of all material functions is excellent.

k	λ_k (s)	a_k (Pa) at 200°C	a_k (Pa) at 215°C	a_k (Pa) at 230°C
1	$1x10^{-4}$	$3.49x10^5$	$2.34x10^5$	$2.10x10^5$
2	$1x10^{-3}$	$1.02x10^5$	84765	97202
3	$1x10^{-2}$	90670	67957	65760
4	$1x10^{-1}$	35247	25051	18627
5	$1x10^{+0}$	5107.8	3167.7	2139.2
6	$1x10^{+1}$	448.12	157.03	121.76
7	$1x10^{+2}$	1.5428	0.13156	0.0633
8	$1x10^{+3}$	0.14936	0.01747	0.01285
		$\alpha = 2.42$	$\alpha = 4.42$	$\alpha = 3.33$
		$\bar{\lambda} = 14.87$ s	$\bar{\lambda} = 4.70$ s	$\bar{\lambda} = 4.65$ s
		$\eta_0 = 14460.8$ Pa·s	$\eta_0 = 8061.5$ Pa·s	$\eta_0 = 6014.4$ Pa·s

Table 2 : Relaxation spectrum and material constants for the polypropylene nanocomposite obeying the K-BKZ model (eqn 8) at different temperatures ($\beta = 0.5$, $\theta = 0$)

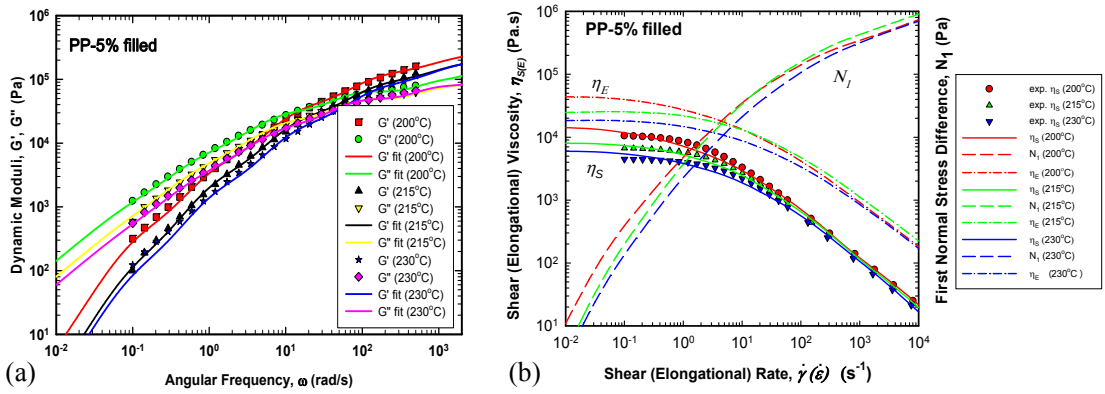

Figure 2. Experimental data (symbols) and model predictions (lines) of the polypropylene nanocomposite using the parameters of Table 2 with the K-BKZ model (eqn 8): (a) storage (G') and loss (G'') moduli, (b) shear viscosity (η_S), normal stresses (N_1), and elongational viscosity (η_E)

3.1 Non-Isothermal Modeling

The non-isothermal modeling follows the one given in earlier publications [18,19] and will not be repeated here. Suffice it to say that it employs the Arrhenius temperature-shifting function, a_T, given by [1,2]:

$$a_T(T) = \frac{\eta}{\eta_0} = \exp\left[\frac{E}{R_g}\left(\frac{1}{T} - \frac{1}{T_0}\right)\right] \tag{12}$$

In the above, η_0 is a zero-shear viscosity at T_0, E is the activation energy constant, R_g is the ideal gas constant, and T_0 is a reference temperature (in K). The activation energy constant E can be determined from the shift factors obtained by applying the time-temperature superposition to get the curves plotted in Figure 2a. It was found to be 53,500 J/mol, typical for a polypropylene resin.

In the present work we have applied the above equation to derive the non-isothermal constitutive equation from the isothermal one. This method is based on the time-temperature superposition principle and simply consists of shifting the relaxation times λ_k from the temperature history within the material's internal time scale t' [18]. The equation used to shift the relaxation times in the material's history is given by [18,19]:

$$\lambda_k\left(T'(t')\right) = \lambda_k\left(T_0\right) a_T\left(T'(t')\right) \tag{13}$$

where T' is the temperature at time t'.

The viscoelastic stresses calculated by the non-isothermal version of the above constitutive equation (eqn 8) enter in the energy equation (eqn 3) as a contribution to the viscous dissipation term.

The thermal properties of the polypropylene nanocomposite are given in Table 3. The various thermal and flow parameters are combined to give appropriate dimensionless numbers [18,19]. The relevant ones here are the Peclet number, Pe, and the Nahme-Griffith number, Na. These are defined as:

$$Pe = \frac{\rho C_p U R}{k} \tag{14}$$

$$Na = \frac{\bar{\eta} E U^2}{k R_g T_0^2} \tag{15}$$

where $\bar{\eta} = f(U/R)$ is a nominal viscosity given by the Cross model (eqn 7) at a nominal shear rate of U/R, and $U\ (=\dot{\gamma}_A R/4)$ is the average velocity in the capillary die. The Pe number represents the ratio of heat convection to conduction, and the Na number represents the ratio of viscous dissipation to conduction and indicates the extent of coupling between the momentum and energy equations. A thorough discussion of these effects in non-isothermal polymer melt flow is given by Winter [20].

Parameter	Value
k	0.18 W/m/K
ρ	0.79 g/cm^3
C_P	2873.25 J/kg/K

Table 3 : Thermal properties of polypropylene nanocomposite

With the above properties and a die radius R=0.075 cm, and for capillary velocities $0.1875 < U < 18{,}750$ cm/s, the dimensionless thermal numbers are in the ranges: $18{,}000 < Pe < 1.8\text{x}10^{+9}$, $1 < Na < 10$, showing a very strong convection (Pe>>1), and also a strong coupling between momentum and energy equations (Na>1). A value of $Na > 1$ indicates temperature non-uniformities generated by viscous dissipation, and a strong coupling between momentum and energy equations.

4 METHOD OF SOLUTION

The solution of the above conservation and constitutive equations is carried out with two codes, one for viscous flows (*u-v-p-T-h* formulation) [21] and one for viscoelastic flows [22]. The boundary conditions (BC) for the problem at hand are well known and can be found in our earlier publications [13,19]. Briefly, we assume no-slip and a constant temperature T_0 at the solid walls; at entry, a fully-developed velocity profile is imposed, corresponding to the flow rate at hand, and a constant temperature T_0 is assumed; at the outlet, zero surface traction and zero heat flux are assumed; at the centerline, symmetry is assumed.

The present work follows along the lines of our recent publication on LDPE [23], where the necessary numerical checks were made for the pressure- and temperature-dependence of viscosity in non-isothermal viscous and viscoelastic flows. The solutions for the viscous flows were checked with both computer codes with identical results. The novelty in the present work is extending the simulations to extremely high apparent shear rates (1,000,000 s^{-1}), something that had not been done before in both the viscous and viscoelastic simulations.

The viscous simulations are extremely fast and are used as a first step to study the whole range of parameter values and die designs. The viscoelastic simulations admittedly are much harder to do and they need good initial flow fields to get solutions at such elevated apparent shear rates as 1,000,000 s^{-1}. In our recent works [14,23], we explained how it was possible for the first time to do viscoelastic computations up to the highest apparent shear rates with good results. Briefly, the solution strategy starts at a given apparent shear rate from the viscous non-isothermal solution, and then using this as an initial solution it continues for the non-isothermal viscoelastic solution with all effects present.

Table 4 shows the apparent shear rate steps required to get the solution at different levels of viscoelasticity with both models (viscous Cross and viscoelastic K-BKZ) in an injection molding die labeled kLr with entrance angle $2\alpha=60^o$. In general, 17 steps were used to start from the lowest apparent shear rate of 5 s^{-1} and reach the highest rate of 1,000,000 s^{-1}. The runs are always fast and well behaved for the viscous case. However, for the viscoelastic case, the runs are fast in the beginning (up to 100 s^{-1}), after which there appears a bottleneck in the solution process with many more iterations needed (up to 1000 s^{-1}), but after that and due to severe shear-thinning of the polymer melt, it appears that iterations are few, the convergence rate is faster, and the solution process is well behaved. Thus, we were able to reach the 1,000,000 s^{-1} mark, something not done before, and with good convergence of the solution. In general, the two solutions and up to 1000 s^{-1} give similar pressure results, but after that the viscoelastic runs give higher pressure drops, reflecting the experimental data in a much better way than the viscous runs.

k	$\dot{\gamma}_A$ *(1/s)*	*P (MPa) at 210°C Viscous Cross Model*	*P (MPa) at 210°C Viscoelastic K-BKZ Model*
1	10	0.86	0.65
2	20	1.23	0.94
3	50	1.78	1.45
4	100	2.20	1.95
5	200	2.67	2.53
6	500	3.38	3.37
7	1,000	3.99	4.19
8	2,000	4.66	5.25
9	4,000	5.37	6.56
10	6,000	5.80	7.43
11	12,000	6.55	9.08
12	18,000	7.00	10.05
13	33,000	7.71	11.38
14	98,000	9.14	13.91
15	150,000	9.76	15.49
16	450,000	11.51	25.09
17	1,000,000	12.23	35.43

Table 4 : Steps for convergence of the simulations at different apparent shear rates in injection molding of polypropylene nanocomposite in die design kLr with entrance angles $2\alpha=60^o$

5 RESULTS AND DISCUSSION

Runs were done first for the capillary dies in which rheological characterization of the polymer took place. The die designs together with the finite element meshes are shown in Figure 3. The domain represents an 12:1 abrupt circular contraction with an entrance angle 2α = 180°. The upper grid consists of 1700 elements, 7161 nodes, and 22,261 unknown degrees of freedom (d.o.f.), while a 4-times denser grid (lower grid) is also used, having been created by subdivision of each element into 4 sub-elements for checking purposes of grid-independent results. This checking consists of reporting the overall pressures in the system from the two meshes and making sure that the differences are less than 1% between the two results. Having fixed the model parameters and the problem geometry, the only parameter left to vary was the apparent shear rate in the die ($\dot{\gamma}_A = 4Q/\pi R^3$). Simulations were performed for the whole range of experimental apparent shear rates in the capillary dies, namely from 10 s^{-1} to as high as 10,000 s^{-1}.

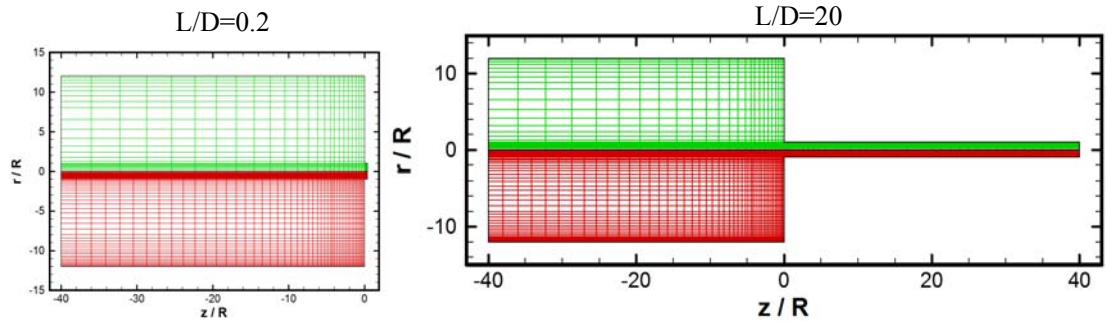

Figure 3. Finite element meshes used in the capillary die simulations with different die lengths *L/D*. The lower half has 4 times the number of elements of the upper half, for comparison purposes of the two meshes

Figure 4a shows the results from the two dies (orifice and long die) at 215°C together with the experimental data up to apparent shear rates of 10,000 s^{-1}. The dashed lines are the results from the viscous Cross model, while the solid lines are the results from the viscoelastic K-BKZ model. We note that the viscoelastic results are much closer to the experimental data, especially for the long die (*L/D*=20), for which the matching is excellent. On the other hand, in Figure 4b the effect of temperature for the long die is excellently captured by the viscoelastic simulations for the 3 temperatures, while the viscous simulations did not show such a good agreement (results not shown).

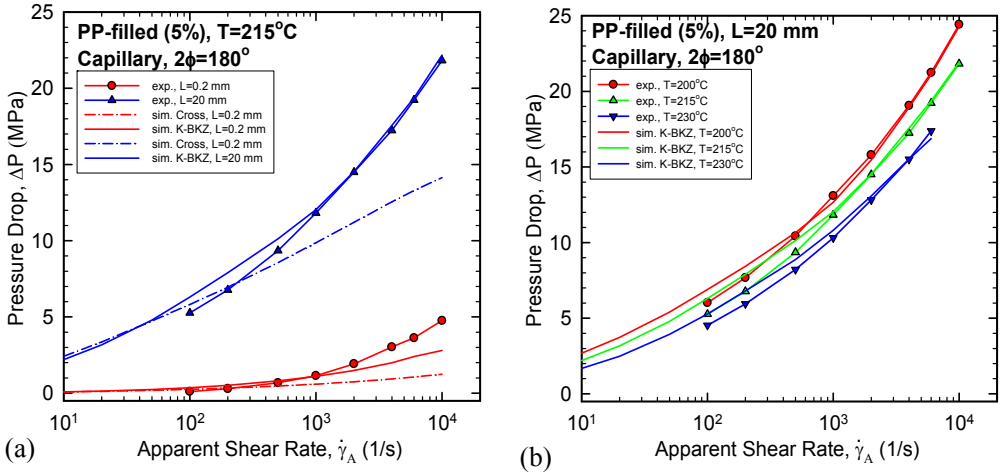

Figure 4. (a) Viscous simulations (dashed lines) and viscoelastic simulations (solid lines) together with experimental data (symbols) for the two capillary dies. (b) Viscoelastic simulations (solid lines) vs. experimental data (symbols) for the three temperatures in the long capillary die

We continue our simulations with the flow of the polypropylene nanocomposite inside injection molding dies, for which there are 4 designs (see Table 5) shown in Figure 5 together with the FEM grids used.

Die Design	Values
kLR	R=0.125 cm, R_{res}=0.5 cm, L/R=5.888, 2α=54°
kLr	R=0.075 cm, R_{res}=0.5 cm, L/R=9.813, 2α=60°
klr	R=0.075 cm, R_{res}=0.5 cm, L/R=3.40, 2α=118°
klR	R=0.125 cm, R_{res}=0.5 cm, L/R=2.04, 2α=111.6°

Table 5 : Die designs for the injection molding equipment

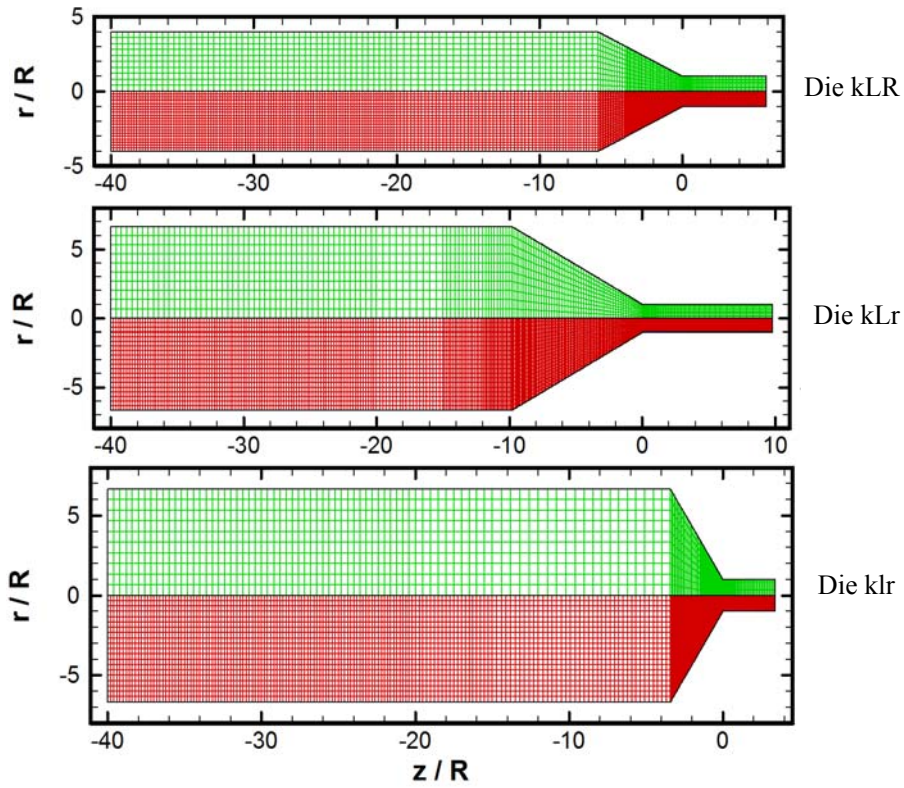

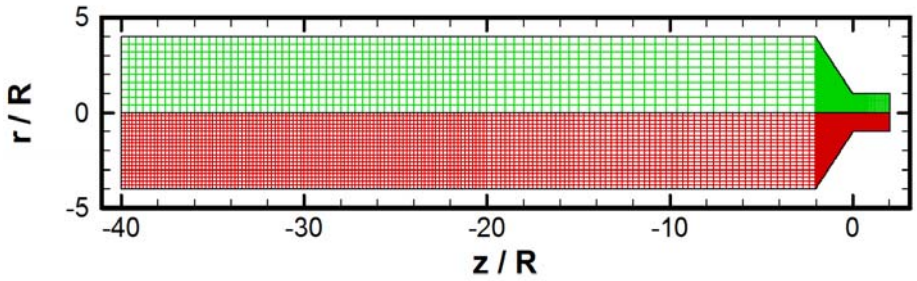

Figure 5. Finite element meshes used in the simulations for the injection molding dies

The runs for these dies go up to 1,000,000 s^{-1}, which is extremely high. The simulations with the viscous Cross model and the viscoelastic K-BKZ model are done with the FEM grids of Figure 5 and for the whole range of experimental data. The results are shown in Figure 6a-d for the 4 designs. It is seen that in all cases the viscous results are severely underestimating the experimental data, while the viscoelastic results show a tendency to get higher pressure drops in the system for apparent shear rates of 1000 s^{-1} and higher. Still though, the experimental data are higher at the extremely high shear rates, something that needs further investigation.

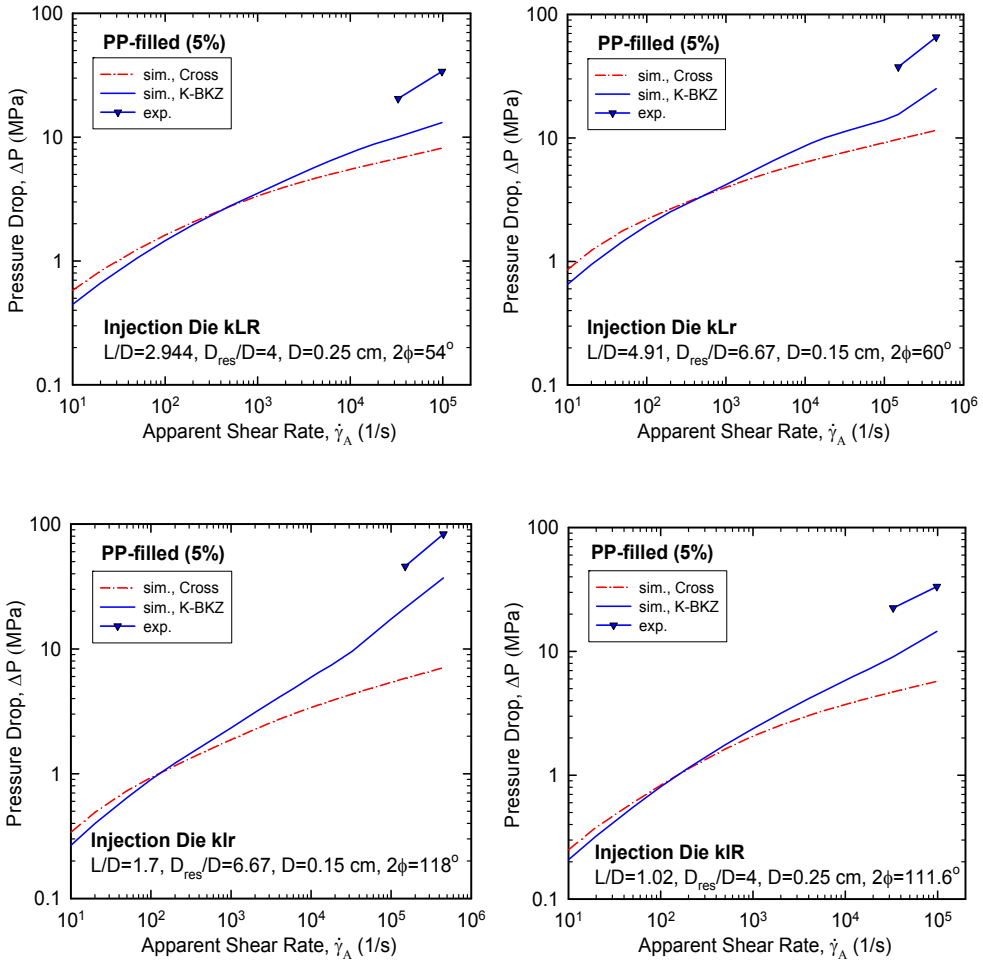

Figure 6. Injection molding data (solid symbols) and model predictions for 4 conical dies at 210°C for the PP-filled melt using the Cross (eqn 7) and K-BKZ (eqn 8) models with the parameters listed in Tables 1 and 2

6 CONCLUSIONS

Numerical simulations have been performed for a polypropylene nanocomposite (5%) first in capillary dies

and then in injection molding dies. The novelty of the simulations is to reach extremely high apparent shear rates (up to 1,000,000 s^{-1}), which had not been done before. The models for the simulations were the viscous Cross model and the viscoelastic K-BKZ model. Whereas for the viscous model, the simulations do not show any difficulties in any value of apparent shear rate, the viscoelastic model showed a bottleneck in the range of 100 s^{-1} to 1000 s^{-1}, after which its convergence was good, due apparently to very high shear-thinning of the material at very high shear rates.

The viscous model usually severely underpredicts the pressure drop in the system, while the viscoelastic model predicts correctly the rheology, and then underpredicts somewhat the pressure drops of the experimental data. Pressure-dependence of the viscosity, not taken into account in the present runs, may be an explanation for these discrepancies, and our future work will concentrate on that aspect of rheology to predict more satisfactorily the experimental data in these difficult experiments.

ACKNOWLEDGEMENTS

Financial support from the Department of Polymer Engineering and Science, Montanuniversität Leoben, Leoben, Austria, is gratefully acknowledged.

REFERENCES

[1] Bird, R.B., Armstrong, R.C. and Hassager, O. (1987), *Dynamics of Polymeric Liquids, Vol. 1, Fluid Mechanics*, 2nd Ed., Wiley Interscience, New York.
[2] Tanner, R.I. (2000), *Engineering Rheology*, 2nd Ed., Oxford University Press, Oxford.
[3] Macosko, C.W. (1994), *Rheology: Principles, Measurements, and Applications*, VCH Publishers, New York.
[4] McLeish, T.C.B. and Larson, R.G. (1998), "Molecular Constitutive Equations for a Class of Branched Polymers: The Pom-Pom Polymer", *Journal of Rheology*, Vol. 42, pp. 82-112.
[5] Kaye, A. (1962), "Non-Newtonian Flow in Incompressible Fluids, Part I: A General Rheological Equation of State; Part II: Some Problems in Steady Flow", *Note No. 134*, College of Aeronautics, Cranford, UK.
[6] Bernstein, B., Kearsley, E.A. and Zapas, L. (1963), "A Study of Stress Relaxations with Finite Strain", *Transactions of the Society of Rheology*, Vol. 7, pp. 391-410.
[7] Wagner, M.H. (1978), "A Constitutive Analysis of Uniaxial Elongational Flow Data of a Low-Density Polyethylene Melt", *Journal of Non-Newtonian Fluid Mechanics*, Vol. 4, pp. 39-55.
[8] Papanastasiou, A.C., Scriven, L.E. and Macosko, C.W. (1983), "An Integral Constitutive Equation for Mixed Flows: Viscoelastic Characterization", *Journal of Rheology*, Vol. 27, pp. 387-410.
[9] Keunings, R. (1986), "On the High Weissenberg Number Problem", *Journal of Non-Newtonian Fluid Mechanics*, Vol. 20, pp. 209-226.
[10] Marchal, J.M. and Crochet, M.J. (1987), "A New Mixed Finite Element for Calculating Viscoelastic Flow", *Journal of Non-Newtonian Fluid Mechanics*, Vol. 26, pp. 77-114.
[11] Luo, X.-L. and Tanner, R.I. (1986), "A Streamline Element Scheme for Solving Viscoelastic Flow Problems, Part II. Integral Constitutive Models", *Journal of Non-Newtonian Fluid Mechanics*, Vol. 22, pp. 61-89.
[12] Mitsoulis, E. (2013), "50 Years of the K-BKZ Constitutive Relation for Polymers", *ISRN Polymer Science*, Hindawi Publishing Corporation, New York, Article ID 952379, pp. 1-22.
[13] Barakos, G. and Mitsoulis, E. (1995), "Numerical Simulation of Extrusion through Orifice Dies and Prediction of Bagley Correction for an IUPAC-LDPE Melt", *Journal of Rheology*, Vol. 39, pp. 193-209.
[14] Ansari, M., Alabbas, A., Hatzikiriakos, S.G. and Mitsoulis, E. (2010), "Entry Flow of Polyethylene Melts in Tapered Dies", *International Polymer Processing*, Vol. 25, pp. 287-296.
[15] Neunhäuserer, A. and Friesenbichler, W. (2014), private communication to the author.
[16] Luo, X.-L. and Tanner, R.I. (1988), "Finite Element Simulation of Long and Short Circular Die Extrusion Experiments Using Integral Models", *International Journal for Numerical Methods in Engineering*, Vol. 25, pp. 9-22.
[17] Kajiwara, T., Barakos, G. and Mitsoulis, E. (1995), "Rheological Characterization of Polymer Solutions and Melts with an Integral Constitutive Equation", *International Journal of Polymer Analysis and Characterization*, Vol. 1, pp. 201-215.
[18] Luo, X.-L. and Tanner, R.I. (1987), "A Pseudo-Time Integral Method for Non-Isothermal Viscoelastic Flows and its Application to Extrusion Simulation", *Rheologica Acta*, Vol. 26, pp. 499-507.
[19] Barakos, G. and Mitsoulis, E. (1996), "Non-Isothermal Viscoelastic Simulations of Extrusion through Dies and Prediction of the Bending Phenomenon", *Journal of Non-Newtonian Fluid Mechanics*, Vol. 62, pp. 55-79.
[20] Winter, H.H. (1977), "Viscous Dissipation in Shear Flows of Molten Polymers", *Advances in Heat Transfer*, Vol. 13, pp. 205-267.
[21] Hannachi, A. and Mitsoulis, E. (1993), "Sheet Coextrusion of Polymer Solutions and Melts: Comparison between Simulation and Experiments", *Advances in Polymer Technology*, Vol. 12, pp. 217-231.
[22] Luo, X.-L. and Mitsoulis, E. (1990), "An Efficient Algorithm for Strain History Tracking in Finite Element Computations of Non-Newtonian Fluids with Integral Constitutive Equations", *International Journal for Numerical Methods in Fluids*, Vol. 11, pp. 1015-1031.
[23] Ansari, M., Zisis, Th., Hatzikiriakos, S.G. and Mitsoulis, E. (2012), "Capillary Flow of Low-Density Polyethylene", *Polymer Engineering and Science*, Vol. 52, pp. 649-662.